applied sciences

MDPI

Article

Effect of Ambient Temperature on Impedance-Based Physiological Activity Evaluation of Zelkova Tree

Jounghoon Lim, Jinkee Kim and Jong Pal Kim *

Advanced Research Center for Mechatronics Engineering, School of Mechatronics Engineering, Korea University of Technology and Education, Cheonan 31253, Republic of Korea; ljhoom9097@koreatech.ac.kr (J.L.); kjkee128@koreatech.ac.kr (J.K.)
* Correspondence: jongpalk@koreatech.ac.kr

Abstract: A system has been developed to remotely, continuously, and quantitatively measure the physiological activity of trees. The developed tree physiological activity monitoring (TPAM) system is equipped with electrical impedance, temperature, and light intensity measurement functions. In the two-contact impedance measurement method used in the previous plant impedance measurement, errors due to the polarization impedance of the electrodes could not be avoided. The developed TPAM system adopted a four-contact measurement method that could avoid polarization impedance errors, and, with it, the long-term monitoring of zelkova trees was performed. The monitoring of seasonal changes was conducted from July to November, and an impedance change pattern that repeated on a daily basis was observed in the short term, and an overall increase in the impedance was observed in the long term. Impedance changes related to daily temperature changes were observed even after all the tree leaves had fallen, meaning that this effect should be excluded when using impedance to evaluate tree vitality. For this reason, the influence of temperature fluctuations was excluded by using only the impedance values at the same daily temperature of 25 degrees from July to November. The analysis results at 25 degrees showed that the tree impedance value increased linearly by 8.7 Ω per day. The results of this series of long-term monitoring and analysis revealed that the ambient temperature must be taken into account in the evaluation of tree physiological activity based on electrical impedance.

Keywords: electrical impedance; tree physiological activity; ambient temperature; continuous monitoring; zelkova

check for updates

Citation: Lim, J.; Kim, J.; Kim, J.P. Effect of Ambient Temperature on Impedance-Based Physiological Activity Evaluation of Zelkova Tree. *Appl. Sci.* **2024**, *14*, 1305. https://doi.org/10.3390/app14031305

Academic Editor: Alessandro Lo Schiavo

Received: 26 December 2023
Revised: 27 January 2024
Accepted: 31 January 2024
Published: 5 February 2024

1. Introduction

Tree physiological activity has traditionally been measured relying on visual observation. The visual observation method sets indicators such as the tree size and crown density, and the observer records qualitative scores for the indicators [1,2]. Figure 1 shows photos of zelkova trees in summer and fall. In the summer, the leaves of the trees are lush and green, and in the fall, the leaves turn brown. In the summer, the physiological activity of the tree will be active, and as the leaves fall in the fall, the physiological activity of the tree will gradually decrease. Because these methods require an observer to intervene and perform visual observations, it is difficult to automate them based on quantitative measurements. Therefore, has become necessary to develop a measuring device to quantitatively evaluate the physiological activity of trees. In 1977, Dr. Shigo developed the Shigometer, a device that measures the resistance of trees to quantify their physiological activity [3]. If a tree's physiological activity is high, the movement of water and electrolyte nutrients between the roots and leaves will become more active. Water and nutrients are transported between the roots and leaves through the xylem and phloem, respectively, in the outer layer of the tree. The xylem and phloem are located on the outside when viewed from the cross-section of the tree trunk, and are formed in a tubular shape in the direction of the tree pillar. Therefore, the physiological activity of a tree can be estimated by measuring the xylem and/or phloem resistance in the direction of the tree trunk. In other words, if the physiological activity of the tree is high, the amount of electrolytes transported will be abundant, so the measured resistance of the tree will be low. If the physiological activity of the tree is low, the amount of electrolytes transported will be low, so the measured resistance of the tree will be high. Figure 2a shows the main body of the Shigometer, and Figure 2b shows the measurement probe inserted into the tree. Shigometers are used to assess the tree's physiological activity by inserting a probe into the tree trunk at an appropriate depth and then reading the numbers displayed on the main device. It can be seen that the probe is firmly mechanically supported after being embedded in the wood tissue. However, because the Shigometer uses a one-time measurement method, it is difficult to expect the same contact impedance when newly inserted for each measurement. The number displayed on the body is the same as the impedance value calculated using the DC current flowing through the probe and the voltage derived from the DC current. Therefore, the higher the level displayed in the body, the lower the physiological activity, and the lower the level, the higher the physiological activity. The Shigometer has also recently been used to measure the physiological activity of trees [4]. The Shigometer uses only two probes and measures the resistance through the flowing DC current. When only two probes are used, errors due to contact resistance components cannot be avoided, and when measuring with only the DC current flowing, the influence of the capacitance components cannot be included. Additionally, when the DC current is used when measuring impedance, a polarization impedance is formed at the interface between the electrode and the ionic solution, affecting the contact impedance [5]. Since measurements are made once by poking the probe into the wood, the contact resistance changes with each measurement, which also deteriorates the measurement reproducibility.

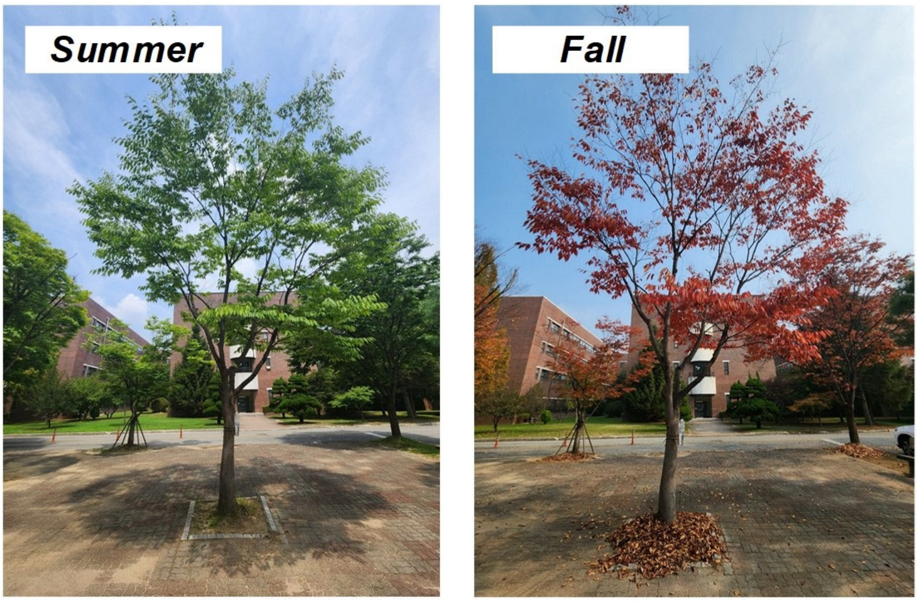

(a) (b)

Figure 1. Appearance of zelkova trees according to the seasons (**a**) summer and (**b**) fall.

Muramatsu N. measured the impedance of small branches before and after dehydration [6]. The tree branch was cut into 3 cm lengths, stainless steel electrodes were placed in surface contact with the cut cross-sections at both ends, and the impedance was measured with an LCR meter. Because the two-contact measurement method was used in the impedance measurement, errors due to the contact impedance of the electrode were not considered. Rafael F. M. measured and published the correlation between the nitrogen content and electrical impedance in lettuce [7]. Two 0.75 cm long stainless steel needles were used as electrodes, and the impedance was measured using an LCR meter. Since the contact area between the needle and the lettuce leaf is small, the contact impedance is expected to be relatively large compared to the impedance of the lettuce leaf. Since the two-contact measurement method was used, a large error due to contact impedance would have been included in the measurement results. Maxim E. A. utilized impedance measurements to monitor the healing process after grafting [8]. The impedance was measured using two nickel sheet electrodes that can cover tree skin up to 45 mm in diameter. Because the electrodes were placed around the outside of the tree bark, the contact impedance of the electrodes would have been very large, and because the two-contact measurement method was used, measurement errors are presumed to have occurred.

(**a**) (**b**)

Figure 2. Shigometer: (**a**) a measuring device and (**b**) probes inserted into a tree.

Since the previously mentioned preliminary studies all used a two-contact impedance measurement method, they could not in principle overcome the error in the contact resistance. There are also examples of the four-point electrical impedance measurement method being applied to plant applications research. Serrano-Finetti E. measured the impedance of leaves cut into 5 cm $\times$ 6 cm pieces using a four-point measurement method six times over two days while they were drying [9]. Meyqing L. used a four-point impedance measurement method using an impedance analyzer (Impedance Interface 1294, Solartron Analytical, Farnborough, UK) to examine the relationship between the phosphoric acid content and impedance of tomato leaves [10]. This study was conducted in an indoor laboratory using devices or instruments and performed four-contact measurements based on intermittent measurements. The previous four-point measurement systems are insufficient in the real-time, long-term impedance monitoring of trees growing in actual outdoor environments, so no continuous long-term impedance monitoring data has yet been reported. To monitor the physiological activity of outdoor trees, a tree physiological activity monitoring system (TPAM) capable of continuous, long-term, four-point impedance monitoring was developed.

The developed TPAM system was mounted on a tree, and the tree impedance was measured continuously from summer to winter. The TPAM system simultaneously measures not only the impedance but also the ambient temperature and illuminance, and the measured data are accumulated in the hub system through Zigbee wireless communication. TPAM is a useful research tool that can obtain biometric and ambient information of trees growing outdoors on a long-term continuous remote basis. TPAM makes it possible to acquire and interpret long-term biological and environmental data on plants in areas where this was previously impossible.

Section 2 explains the difference between the two-contact impedance measurement method and the four-contact impedance measurement method, and Section 3 describes the hardware and software that make up the TPAM system. Section 4 presents the results of the tree impedance long-term monitoring using the developed TPAM system and discussions on the results, and Section 5 concludes.

2. Impedance Measurement Method

Impedance can be calculated by applying a current to the object being measured and measuring the voltage induced in the object being measured. Since the wood and the contact surface between the wood tissue and the measurement probe are expected to be composed of a combination of resistance and capacitance, the impedance measurement is performed using a flowing AC current rather than a DC current.

Figure 3a shows the Hayden model, which is often applied as an electrical equivalent model for plant cells [11,12]. The Hayden model represents a tree cell as three resistors and one capacitor. The symbol R_I represents the intercellular resistance and the symbol R_E represents the extracellular resistance. The symbol R_M represents the membrane resistance and the symbol C_M represents the membrane capacitance. The cell membrane is modeled as a parallel combination of capacitance C_M and resistance R_M, the inside of the cell is modeled as a series-connected resistance value R_I, and the material between cells is modeled as a resistance R_E. Previous Shigometers were only able to measure impedance of DC currents, but since tree tissue can be modeled as a combination of resistance and capacitance, the TPAM system requires the ability to change the frequency of the applied current. To measure impedance, a probe is inserted into the tree, and a contact impedance is formed between the metal probe and the tree tissue, as shown in Figure 3b [13]. The symbol C_{PA} represents the interface capacitance, the symbol R_{ct} represents the charge transfer resistance, and the symbol R_S represents the solution resistance. The contact impedance Zc, which is composed of a combination of these components C_{PA}, R_{ct}, and R_S, exists between the probe and the tree tissue. In the two-point impedance measurement method, the contact impedance Z_c component is included, so additional error cannot be avoided.

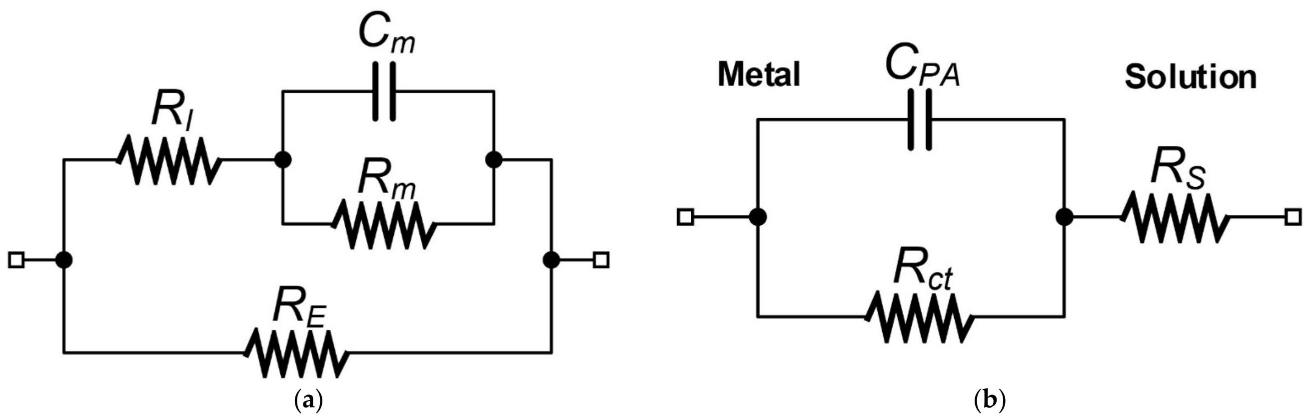

Figure 3. Electrical impedance model: (**a**) Hayden model and (**b**) electrode–electrolyte interface model.

Figure 4a shows the electrical model when measuring the impedance of a tree using the two-point measurement method. The impedance to be measured in the tree is denoted as Z_t, and the contact impedance between the probe and the tree tissue is denoted as Z_{c1} and Z_{c2}. There is also a resistance component of the probe itself, which is connected in series to the measuring instrument, but the resistance of a probe made of metal is so small that it is negligible compared to the contact impedance. Therefore, for simplicity, Z_{c1} and Z_{c2} were not drawn across the border between the probe and the tree, but were drawn as if they were the impedance of the probe itself. The current I_d applied from the current source flows through the contact impedance Z_{c1}, the tree impedance Z_t, and the contact impedance Z_{c2} connected in series between nodes *M1* and *M2*. The voltage measured between nodes *M1* and *M2* also includes contact resistance in addition to the wood impedance, but there is no way to separate the values corresponding to these components. For these technical reasons, traditional Shigometers using a two-point measurement method are bound to be inaccurate. Moreover, when a single measurement is repeated, such as with the Shigometer, the state of the interface between the probe and the tree changes, so the contact impedance value also changes, which inevitably reduces the measurement reproducibility.

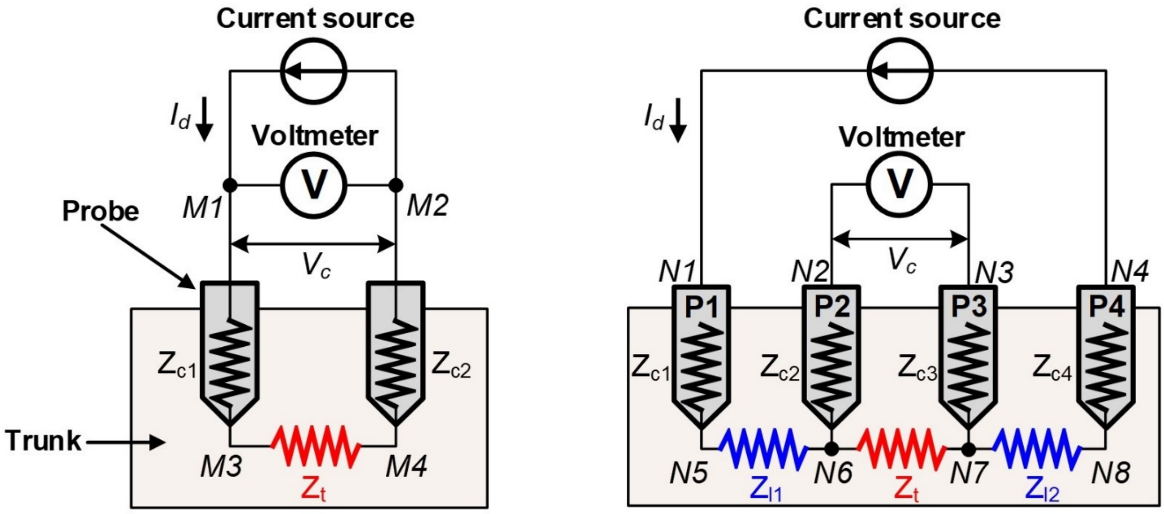

(**a**) (**b**)

Figure 4. Impedance measurement method: (**a**) 2-point measurement method and (**b**) 4-point measurement method.

Figure 4b is an electrical model showing the four-point impedance measurement method. This method flows current I_d through probes P1 and P4 on the outside and measures the voltage through probes P2 and P3 on the inside. The symbol Z_{l1} represents the tree impedance formed between nodes *N5* and *N6*, and the symbol Z_{l2} represents the tree impedance formed between nodes *N7* and *N8*. Since the input impedance of a voltmeter is ideally infinite, the voltmeter between nodes *N2* and *N3* can be modeled as disconnected. Therefore, the path from *N6* through *N2* and *N3* to *N7* is broken, and no current flows along this path. Then, the current I_d supplied from the current source flows entirely through Z_{c1}, Z_{l1}, Z_t, Z_{l2}, and Z_{c4}. Between nodes *N6* and *N7*, the voltage V_t generated by the known current I_d and the measurement target Z_t is formed. Since no current flows between nodes *N6* and *N2*, the voltage at node *N6* is equal to the voltage at *N2*. Likewise, since no current flows between nodes *N7* and *N3*, the voltage at node *N7* is the same as the voltage at *N3*. As a result, the voltage V_c measured at nodes *N2* and *N3* becomes the same voltage as the voltage V_t formed across Z_t. The impedance calculated from the applied current I_d and the measured voltage V_c is related only to the tree impedance Z_t. Therefore, using the four-point measurement method, accurate impedance measurement is possible, excluding the influence of contact impedance. Contact impedance specifically includes the electrode polarization impedance at the interface with the ionic solution for metal electrodes carrying current [14]. Since this polarization impedance occurs at the electrode through which the current flows, the influence of polarization impedance can be avoided by using a four-point measurement method that measures the voltage at a separate electrode [15–17]. Even if a one-time measurement is repeated, the measurement reproducibility is good because the contact impedance value between the probe and the object is not reflected in the measurement value. The four-point measurement method is used in the semiconductor field to accurately measure the surface resistance of wafers without probe contact resistance error [18]. Therefore, the TPAM system being developed must basically have a four-point impedance measurement function.

3. Tree Physiological Activity Monitoring System

A TPAM system to monitor the relationship between tree vitality and tree impedance in the long term is developed. The developed TPAM system can continuously measure the ambient temperature, light intensity, and tree impedance. The measured data are transmitted to the hub via wireless communication. A solar-energy-harvesting function is added to maximize the battery operating time. This section explains the hardware and software configuration of the TPAM system, presents evaluation results to verify its performance, and explains the installation configuration on a zelkova tree.

3.1. TPAM System Hardware

Figure 5a shows the top diagram of the TPAM system. The system consists of two parts: the on-tree system and the hub system. The on-tree system is attached to a tree and measures various data and transmits it to the hub system. The hub system receives measured data, displays it on the graphic user interface (GUI), and stores it in the storage device.

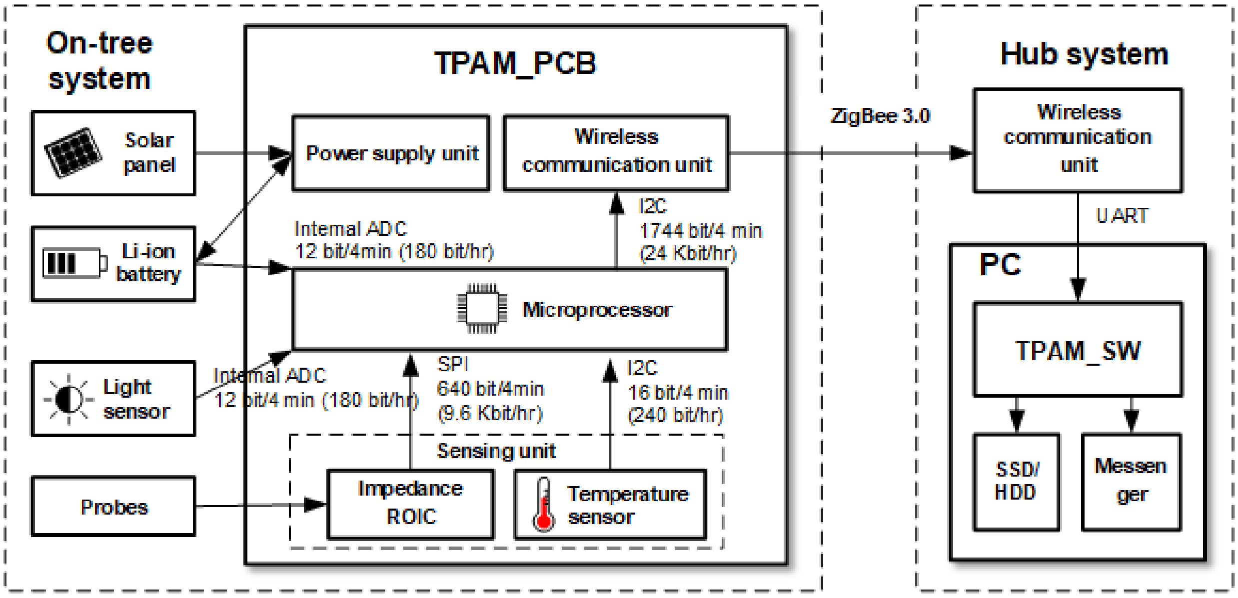

(**a**)

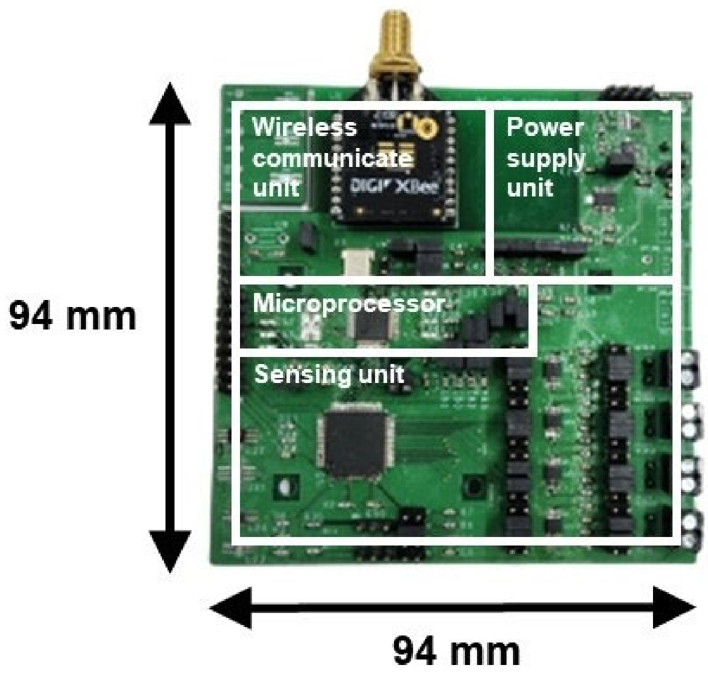

(**b**)

Figure 5. Tree physiological activity monitoring (TPAM) system: (**a**) top block diagram of TPAM system and (**b**) implemented PCB (TPAM_PCB).

The on-tree system consists of a measurement board (TPAM_PCB), a battery, and components located outside the measurement board (solar panel, light sensor, probes).

The measurement board TPAM_PCB consists of a power supply unit, a sensing unit, a microprocessor, and a wireless communication unit. The solar cell harvesting chip in the power supply unit receives power from the solar panel and charges the battery. And the DC/DC converter and low dropout regulator (LDO) in the power supply unit receive power from the battery and generate various operation voltages required in the measurement board. The sensing unit consists of an on-chip temperature sensor and an impedance readout integrated circuit (ROIC). The microprocessor receives a detection signal from the optical sensor and performs analog-to-digital conversion every 4 min using an internal 12-bit analog-to-digital converter (ADC). The microprocessor also receives detection signals from the battery and performs analog-to-digital conversion every 4 min using an internal 12-bit ADC. The microprocessor receives 16-bit sensing data from the temperature sensor every 4 min via inter-integrated circuit (I2C) communication. The microprocessor receives sensed data from the impedance ROIC every 4 min via serial peripheral interface (SPI) communication. The impedance ROIC was implemented with a commercial chip (AFE4300) and includes current injection, voltage sensing, demodulation, and 16-bit digital conversion functions. The impedance ROIC generates 16 bits of data for each of the five channels, CH1 through CH5. In CH1 and CH2, impedance data are generated using the two-point and four-point measurement methods, respectively, using a probe inserted to a depth of 6 mm. In CH3 and CH4, impedance data are generated using the two-point and four-point measurement methods, respectively, using a probe inserted to a depth of 13 mm. CH5 generates impedance data measured from a standard resistor mounted on the TPAM_PCB. Additionally, all channels (CH1 to CH5) generate impedance data for the current injection at four frequencies (8 kHz, 16 kHz, 32 kHz, and 64 kHz). When the microprocessor writes a specific register combination to the impedance ROIC, the impedance ROIC outputs a current of 8 kHz, measures the data on CH1, and transmits the data to the microprocessor. When transmitting data from the impedance ROIC to the microprocessor, a total of 32 bits of data are transmitted, including 16 bits of the reference resistance measurement value and 16 bits of the impedance measurement value measured at 8 kHz in CH1. Immediately after that, when the microprocessor writes another specific register combination to the impedance ROIC, the impedance ROIC outputs a current of 16 kHz, measures the data on CH1, and transmits the data to the microprocessor. Then, when data are transmitted from the impedance ROIC to the microprocessor, a total of 32 bits of data are transmitted, including 16 bits of the reference resistance measurement value and 16 bits of the impedance measurement value measured at 16 kHz on CH1. In this way, 32 bits of data are generated for five channels and four injection current frequencies every 4 min, collecting a total of 640 bits of data. Whenever new data are collected from each sensor, the microprocessor constructs a data packet and transmits it to the wireless communication unit through I2C communication. The wireless communication unit transmits the data packet received from the microprocessor to the hub system using ZigBee wireless communication. The data packet constructed by the microprocessor consists of an 8-bit header (0xE7), 8-bit data ID, 8-bit data length, pay load, and 8-bit tail (0xE7). The length of the pay load consists of 48 bits for the impedance sensor, and 16 bits for the optical sensor, temperature sensor, and battery voltage level. The 48-bit payload for the impedance sensor consists of a 16-bit reference value, 16-bit channel measurement value, 8-bit channel information, and 8-bit injection current frequency information. The 16-bit payload of a temperature sensor consists of all 16 bits of the temperature value. The 16-bit payload of the optical sensor and battery voltage level consists of both 4 bits of dummy data and 12 bits of sensor value.

The hub system consists of a ZigBee wireless communication module and software (TPAM_SW) for the TPAM system. The PC program TPAM_SW extracts sensor data from wirelessly transmitted data packets, rearranges them in chronological order for each sensor, plots them on the screen, and saves them as a file in the storage device. Additionally, if there is no wireless transmission continuously for a preset number of times, a function is implemented to send a system error message to the administrator. The PC program TPAM was developed in-house based on MATLAB R2023a.

Figure 5b shows the implemented measurement board. The size of the board is 94 mm wide and 94 mm tall. The main blocks of the measurement board, which are the power supply unit, sensing unit, microprocessor, and wireless communication unit, are marked with boxes. Table 1 shows the supply voltage and current consumption of TPAM system. the fabricated TPAM system operates at 5 V and consumes 172.5 mW of power. The main units, the sensing unit, microprocessor, and wireless communication unit, were measured to consume a power of 36 mW, 22.5 mW, and 106.5 mW, respectively.

Table 1. Power consumption of TPAM system.

Units	Supply Voltage	Current Consumption	Power Consumption
Power supply (total)	5 V	34.5 mA	172.5 mW
Sensing unit	5 V	7.2 mA	36.0 mW
Microprocessor	5 V	4.5 mA	22.5 mW
Wireless communication unit	5 V	21.3 mA	106.5 mW

To measure the tree impedance, four probes were connected to the measurement board. The probe is made of gold-plated Cu, and has a length of 33 mm and a diameter of 1 mm. The corrosion-resistant nature of gold makes it a suitable metal for long-term monitoring applications. When probes are used in the four-point measurement method, current is passed through two probes and the voltage difference between the remaining two probes is measured. On the other hand, when a probe is used in a two-point measurement method, current flows through two probes and the voltage difference between the two probes through which current flows is measured, and the remaining two probes are not used.

3.2. TPAM System Software

Figure 6a shows the PC software (TPAM_SW) block diagram of the TPAM system. TPAM_SW consists of a communication unit (U_COM), data processing unit (U_DP), data buffer unit (U_DB), alert generation unit (U_ALRT), data-to-storage unit (U_STRG), and graphic user interface unit (U_GUI). Figure 6b shows a PC screen capture corresponding to the U_GUI unit. If the user sets the serial port number and baud rate in the U_GUI unit, the U_COM unit connects to the ZigBee module to receive wireless data and transmit it to the U_DP unit. The U_DP unit interprets the data ID of the received data packet and recognizes which sensor the packet is related to. Then, information is extracted from the pay load and the data are stored in time order in each corresponding sensor buffer in the U_DB unit. The U_DB unit contains data buffers related to the impedance, temperature, light intensity, and battery voltage. Specifically, the impedance buffer consists of separate buffers for each channel and injection current frequency. Data from each sensor stored in the U_DB unit are displayed in the graph window of the U_GUI unit. Referring to the conditions specified in the U_GUI unit, the U_STRG unit can save the data of the U_DB unit to a storage device such as a solid-state drive (SSD) or hard disk drive (HDD). The classified sensing values are saved in Excel format along with time information. The U_ALRT device detects if there is an error in the wireless data reception and sends a message to the designated user's mobile phone. Malfunctions in the TPAM system can be detected remotely, enabling an immediate response if a problem occurs in the TPAM system, enabling continuous, uninterrupted monitoring. The software (TPAM_SW) can connect to and receive data from up to five on-tree systems.

Figure 6b shows the GUI image of TPAM_SW. The GUI consists of a serial port control region, data graph region, and data storage control region. In the serial port control area, users can set the serial port number and baud rate to which the wireless receiver is connected, and control the serial port connection. When the serial port is properly connected, "Connected!" will appear in the headline, allowing users to check the serial port connection status. The data graph region visually displays the impedance, temperature, light intensity, and battery voltage of the four channels. This region displays data in real time and supports zooming in or out via mouse control. In the data storage control region, users can specify the path to save the data, file name, and number of data samples to save. Additionally, log messages that occur during TPAM_SW operation can be saved as a logfile. To avoid situations where there is too many data in one file or it is open for a long time, the file is automatically divided and saved when the amount of data reaches a preset number.

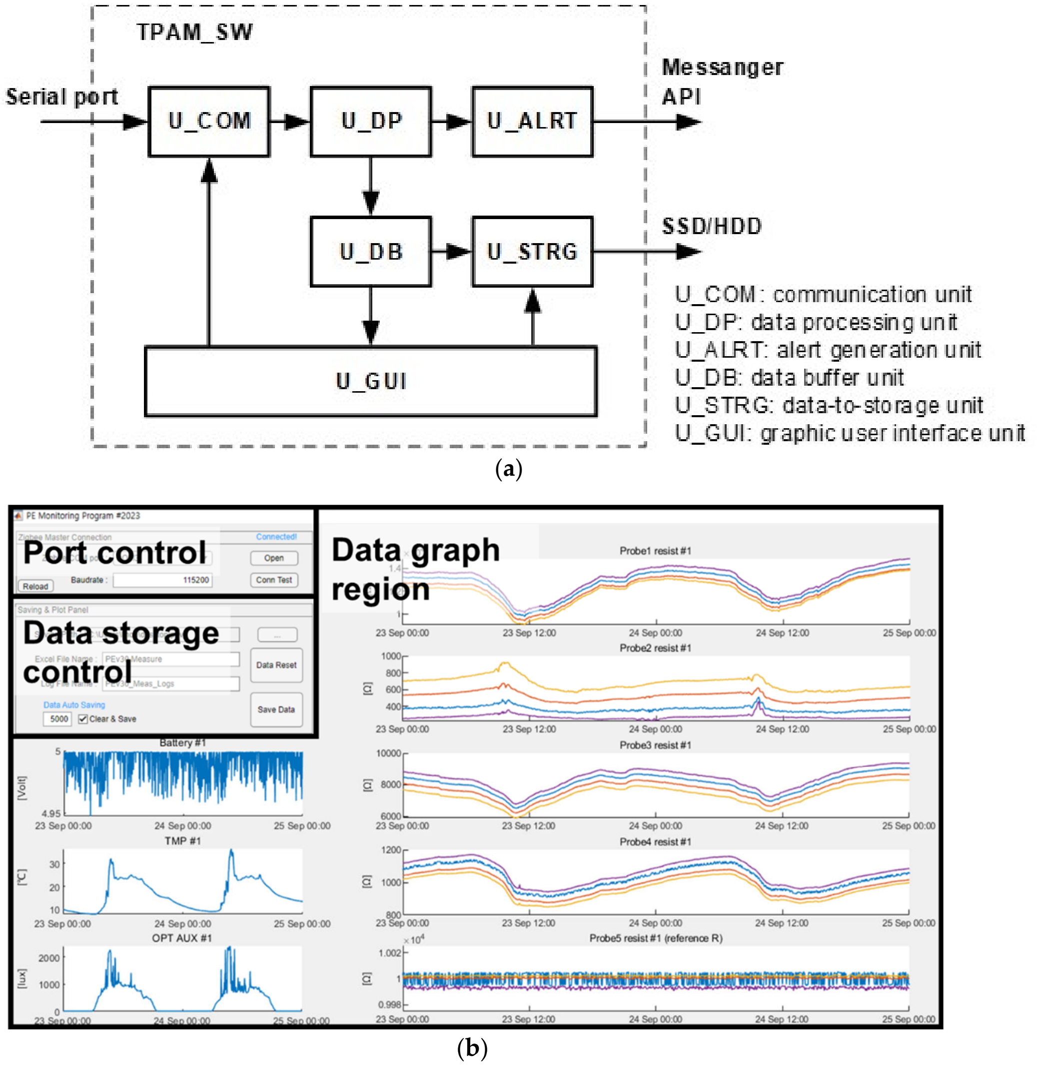

Figure 6. Data acquisition and flow in TPAM system: (**a**) overall flow configuration and (**b**) GUI configuration screen.

3.3. TPAM System Evaluation

Since bioimpedance can be modeled as a combination of a resistor and a capacitor, the TPAM system was evaluated using an idealized resistor and capacitor. Figure 7 shows the measurement results of the TPAM system obtained using ideal components.

Figure 7a shows the resistance value measured using the TPAM system. The x-axis represents the resistance values measured with a standard device (34470A, Keysight, Santa Rosa, CA, USA), and the y-axis represents the values measured with the TPAM system. When measuring in the TPAM system, the frequency of the injection current was changed to 8 kHz, 16 kHz, 32 kHz, and 64 kHz. Even if the frequency of the injection current changes, the measured value remains approximately the same, which is in good agreement with the original characteristics of the resistor. The variation in the resistance value measured according to the frequency is approximately $\pm 30\ \Omega$ at most. In the 1 kΩ to 15 kΩ range, it showed a full-scale nonlinearity of 2.1% and in the 1 kΩ to 8 kΩ range, it showed a full-scale nonlinearity of 1.1%. The straight line is a curve fitting the line of the resistance value measured with the reference device (Keysight 34470A).

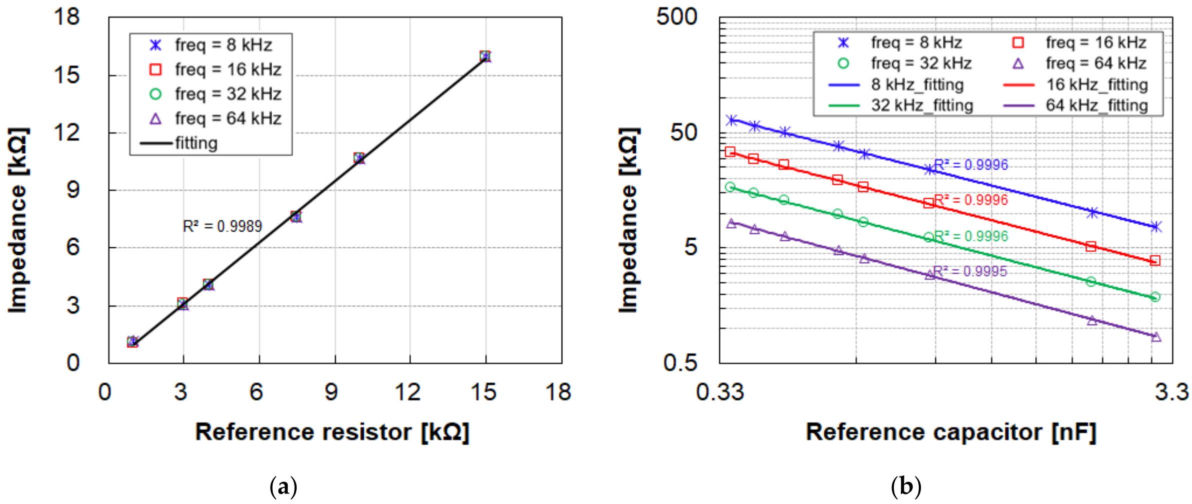

Figure 7. TPAM system evaluation (**a**) with known resistance and (**b**) with known capacitance.

Figure 7b shows the capacitance value measured using the TPAM system. The x-axis represents the capacitance values measured with a standard device (Keysight 34470A) in a logarithmic scale, and the y-axis represents the values measured with the TPAM system in a logarithmic scale. When measuring in the TPAM system, the frequency of the injection current was changed to 8 kHz, 16 kHz, 32 kHz, and 64 kHz. In theory, the impedance of a capacitor is inversely proportional to the capacitance, so when drawn on a logarithmic scale, it is expressed as a straight line with a negative slope. When the capacitance increases from 0.33 nF to 3.3 nF, the measured impedance values in the TPAM system plot as a negative straight line on a logarithmic scale, as expected from theoretical predictions. Also, theoretically, capacitance is inversely proportional to frequency, so the capacitance should be halved every time the frequency is doubled. Looking at the TPAM capacitor measurement results in Figure 7b, you can see that when the frequency value of the injection current is doubled, the impedance value is reduced to 1/2. The straight line in Figure 7b represents the curve-fitted impedance value based on the reference capacitor and frequency.

3.4. TPAM System Application to Tree

The developed TPAM system was applied to the long-term monitoring of zelkova trees. Figure 8 shows the configuration of the TPAM system mounted on a tree and a measurement being conducted. Figure 8a shows the tree being measured and the TPAM system mounted on the tree. The diameter of the tree was measured at 21.6 cm at a height of 1.2 m above the ground. The box containing and protecting the measurement board was installed facing southwest. The use of an opaque box prevents direct sunlight from affecting the temperature sensor on the measurement board. To maximize solar harvesting, solar panels can be placed on the tops of trees or in front of tree trunks so they receive ample sunlight. Since the light intensity sensor must be installed in a place that receives light well, it is also installed where the solar panel is located. Figure 8b shows the inside of the TPAM system box mounted on a tree. A Li-ion battery with a capacity of 5000 mAh is also installed in the system box. The antenna and probe connection cables are routed out of the box through a hole in the bottom, which helps keep it waterproof. Figure 8c shows the probe inserted into the tree. A total of eight probes were installed in a four by two array at a north-facing point. The distance between the two probe columns is 15 mm, and the four probes in one column on the left are inserted to a depth of 13 mm, and the four probes in the other column on the right are inserted to a depth of 6 mm. To remove the impact on the impedance measurements if the probes become wet due to rain, the exposed areas are coated with photosensitive epoxy for electrical insulation. If the diameter of the tip of the probe inserted into the tree is excessively large, cracks may occur in the tree at the insertion point. If a crack occurs at the insertion site, a void is created between the probe and the wood tissue, preventing complete contact between the probe and the wood tissue. Additionally, since the tissue at the crack area is exposed to the outside, the area may dry out or rot, making proper long-term impedance monitoring difficult. Therefore, care must be taken to avoid cracking the wood by inserting the probe, and in this study, a probe with a tip diameter of 1 mm was used. Since the needle probe is tightly clamped by the pressure of the dense tree tissue, the contact between the probe and the tree is solid, and no abnormalities in the insertion state, such as the probe falling out, occur even after several seasons.

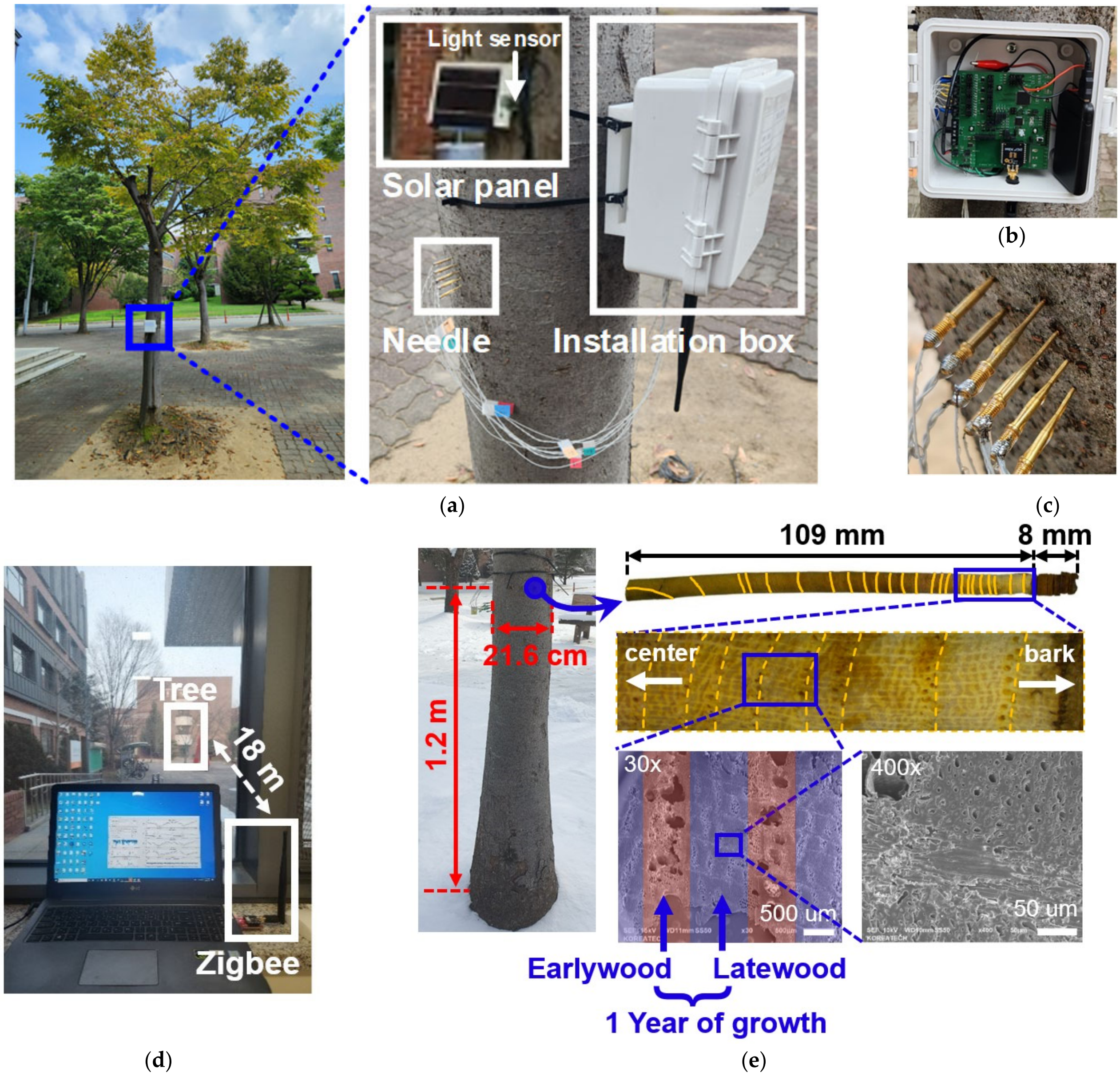

Figure 8. Application configuration of TPAM system: (**a**) zelkova tree to be measured and installed TPAM system, (**b**) TPAM hardware box and built-in PCB, (**c**) inserted probes, (**d**) hub, (**e**) zelkova core samples and growth rings.

The hub shown in Figure 8d is located indoors, 18 m away from the tree where the TPAM hardware is installed. The wireless communication antenna and ZigBee module plugged into the laptop are shown. The GUI of the TPAM software 1.0 is displayed on the laptop screen, and measurement data are received in real time and a graph is plotted.

Figure 8e shows a core sample of a tree collected to determine the tree's age. The age of a tree can be determined from the number of growth rings formed on the cross section of the tree. A tree ring sample was taken at a height of 1.2 m above the ground, towards the center of the tree cross section. The tree ring sample is a thin, cylindrical shape with a diameter of 5 mm and a length of 11.7 cm. The repeating rings of a tree are made up of two parts: early wood and late wood. Each year in the spring and early summer, trees grow rapidly, forming broad, bright early wood sections, while in late summer and fall, trees grow more slowly, forming dark, narrow late wood sections. In the enlarged scanning electron microscope (SEM) image, it can be seen that the early wood region is porous and the late wood region is dense. Since 25 tree rings were found in the obtained tree ring sample, it can be seen that the trees observed in this paper are at least 25 years old.

4. Monitoring Results and Discussion

In this section, the long-term monitoring data using the TPAM system are presented and discussed. The location of the monitoring tree is 36.7650225 latitude and 127.2797814 longitude. The monitoring was conducted from spring (May), when the leaves on the trees were in full bloom, to fall (November), when all the leaves on the trees had fallen. After the wood tissue is damaged by inserting the probe into the tree, the impedance is expected to change as the area where the probe was inserted heals over time. To observe these changes, the impedance change over time after inserting the probe is observed. In the cross-sectional structure of a tree, a significant portion close to the center is dead tissue, and an active layer related to growth exists on the epidermis side. It can be expected that the impedance will vary depending on the depth of the insertion of the probe. Therefore, it is necessary to observe how the impedance changes depending on the insertion depth of the probe. It is clear that the tree growth is affected by the environment temperature and the light of the surrounding environment. It is necessary to examine whether the measured tree impedance is influenced solely by the tree's physiological activity or is also directly influenced by the environment temperature. This can be found by looking at changes in the tree impedance throughout the day when there are no leaves. If the tree impedance value changes during the day even though there are no leaves, it can be said that it is directly affected by temperature. To examine these details, the tree's impedance, environmental temperature, and light intensity were monitored in the long term for several months.

Figure 9 shows the data on the tree impedance, ambient temperature, and solar intensity observed for about four months from July 25 to November 30. As the season changes from summer to fall, changes in the temperature and impedance can be seen. As shown in Figure 9a, the ambient temperature ranges from 20 to 30 degrees in summer in July and August, 10 to 20 degrees in October in early fall, and 0 to 20 degrees in November in late fall. In November, late fall, there is a large daily temperature range with a temperature fluctuation range of up to 20 degrees. Figure 9b shows the simultaneously measured light intensity, and seasonal variations at the macro scale are not clearly visible. As shown in Figure 9c, the impedance has a value of less than 1 kΩ in July and August in the summer, increases to a value of about 1.5 kΩ in October in early fall, and even increases to 2.5 kΩ in November in late fall. During the summer, the impedance change was small, but as late fall approached, the impedance change can be seen to increase. When comparing Figure 9a,c, the change in the impedance depending on the season appears to be related to the change in temperature. The correlation between the temperature and impedance will be discussed in more detail later.

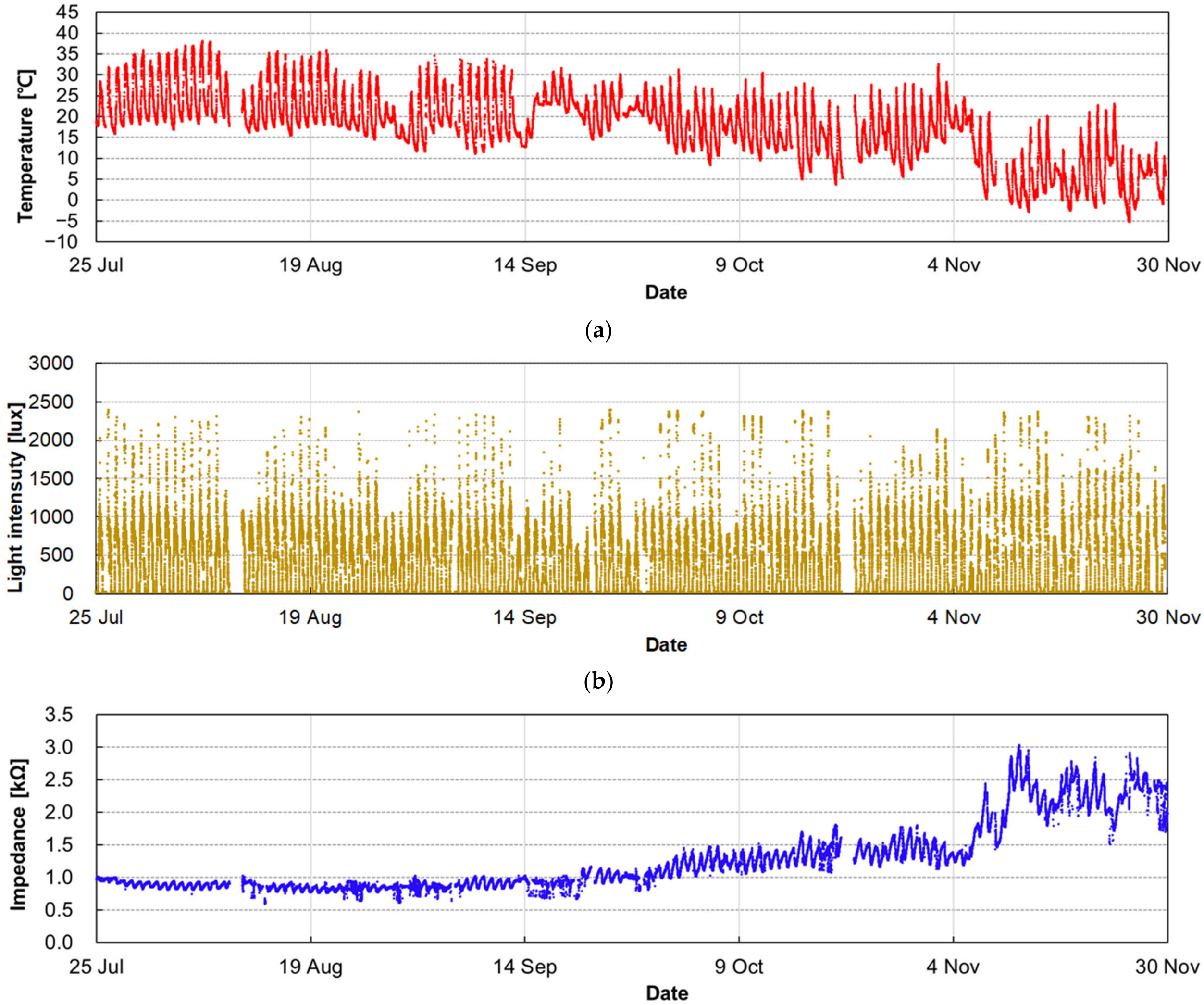

(c)

Figure 9. Long-term observed data: (**a**) ambient temperature, (**b**) light intensity, (**c**) impedance (four-point measurement method).

4.1. Tree Impedance Change after Probe Insertion

Figure 10 shows the change in the impedance over 14 days immediately after inserting the probe into the zelkova tree. The x-axis represents the date and the y-axis represents the tree impedance measured using the four-point measurement method. Immediately after inserting the probe on 31 May, the impedance value was at the 1100 Ω level, and after the overall impedance value decreased for about a week, the impedance value was stable at the 900 Ω level. The tree impedance begins to decrease for 3 to 4 days after the probe is inserted, and the regular pattern of impedance variation that repeats on a daily basis does not appear. Afterwards, a pattern of impedance variation that repeats on a daily basis gradually begins to appear, and after 9 June, 10 days after the insertion of the probe, an impedance variation pattern that repeats on a daily basis is visible. At this time, the tree impedance has a value between approximately 800 Ω and 950 Ω. This tendency is presumed to be a phenomenon that occurs as the tissue around the probe heals over time after the tree tissue is damaged when the probe is inserted into the tree [19]. The closure effect resulting from the healing process can facilitate proper contact between the probe and the tree, ensuring effective connectivity. Considering these observations, it can be seen that the tree impedance information is only reliable if the data are used about a week after probe insertion. Therefore, it is questionable whether a one-time tree impedance measurement using a conventional Shigometer provides appropriate data.

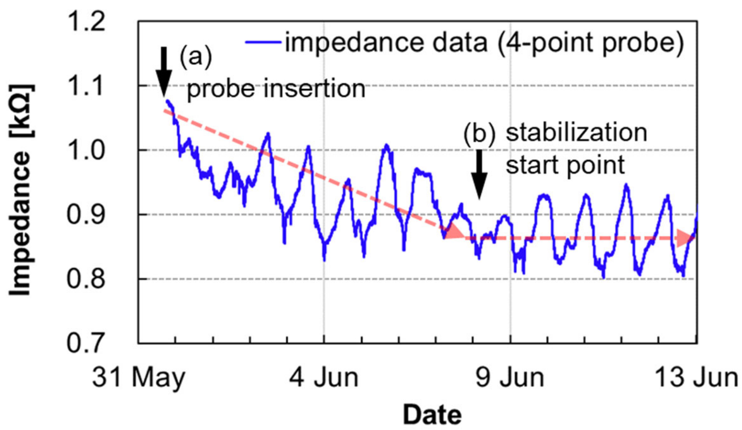

Figure 10. Impedance change over 14 days after insertion of measurement probe.

4.2. Tree Impedance Depending on Probe Insertion Depth

Figure 11 shows a graph of the normalized impedance of the zelkova tree according to the probe insertion depth. The insertion depth of the probe varied from 5 mm to 30 mm at 1 mm intervals. Since the tree impedance was measured using a DC current using a reference instrument (B2912B, Keysight, Santa Rosa, CA, USA), the measured values refer to the resistance. To show the relative ratio rather than the absolute value, it was normalized and expressed based on the resistance value of 13.7 kΩ at a depth of 9 mm. The impedance tended to decrease as the probe was inserted deeper. Since the results were measured using the four-point method, the impedance may not have decreased because the contact area of the probe increased in proportion to the insertion depth. The probe insertion depth of up to 7 mm corresponds to the tree bark, so the impedance value is relatively high. The region with an insertion depth of 7 mm to 13 mm is where the phloem, cambium, and xylem are located, and since these structures are involved in the physiological activities of the tree, the impedance measurement in this region is appropriate. Water is delivered from the roots to the leaves through the xylem, and nutrients are delivered through the phloem. The region exceeding the probe insertion depth of 13 mm corresponds to the sapwood of the tree, the impedance of which gradually decreases with increasing depth. Since the physiological activities of trees occur in the cambium, electrical impedance measurements should also be performed in the cambium [20].

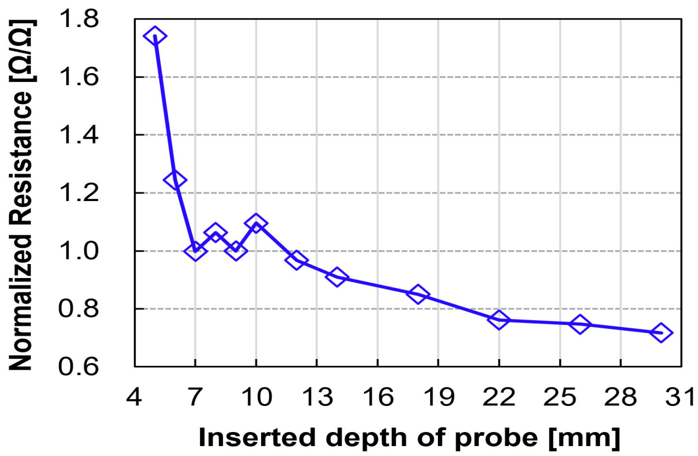

Figure 11. Tree resistance as a function of insertion depth (Keysight B2912B).

4.3. Impedance Trend According to Seasonal Change

Figure 12a shows the impedance data of the zelkova trees measured from September to November and photos of the target trees on specific dates. Figure 12b shows an image of a zelkova tree taken on 24 September, and it was observed that some of the tree's leaves were starting to change color, as shown in the partially enlarged photo. When the color of the leaf begins to change, it means that the exchange of substances with the leaf stops and stem resistance increases. In the impedance graph in Figure 12a, a change in the impedance trend is also visible, as shown at point AA. As summer gradually turns into fall, the leaves of the trees change from green to brown, as shown in Figure 12c on 11 October. Figure 12d shows a photo of a zelkova tree taken on November 5, showing that all of its leaves have fallen. This can also be interpreted in relation to the sharp increase in the impedance levels in early November, at the time indicated by BB in Figure 12a. Therefore, overall, the change in the electrical impedance of the trees can be seen to be linked to changes in the leaves on the trees depending on the season.

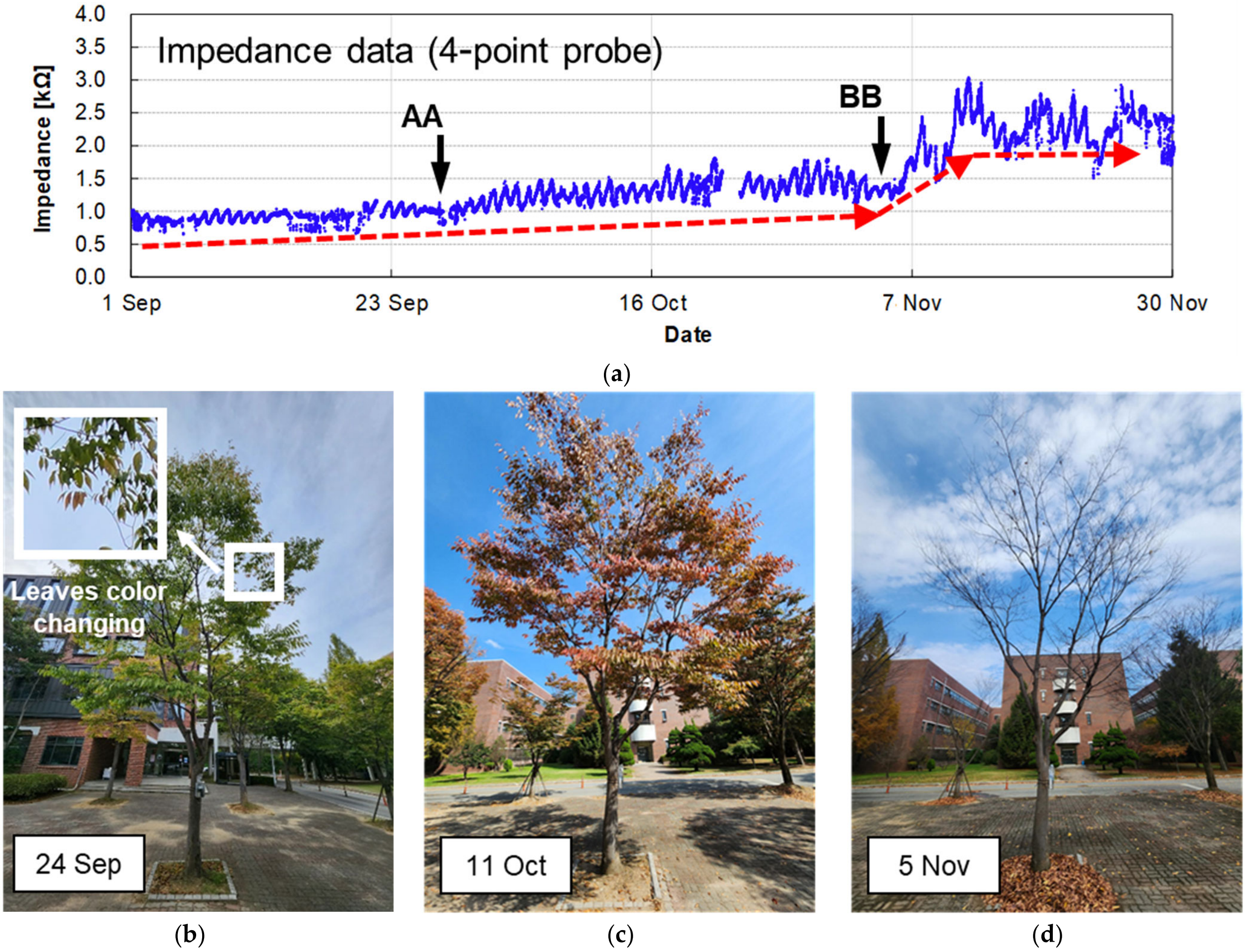

Figure 12. Long-term monitoring of zelkova tree during seasonal changes: (**a**) impedance data measured using the 4-point probe method, (**b**–**d**) appearance of zelkova tree according to seasonal changes.

4.4. Relationship between Ambient Temperature Change and Impedance Change

Figure 13a shows graphs of the temperature and tree impedance data measured from 3 August to 9 August, when the tree was in full leaf. The left y-axis represents the impedance value and the right y-axis represents the ambient temperature value. The lower line is the impedance data and has values ranging from approximately 0.8 kΩ to a maximum of 0.95 kΩ, and the ambient temperature fluctuates in the range of approximately 17 to

36 degrees. In general, as the temperature increases, the impedance tends to decrease, and as the temperature decreases, the impedance tends to increase. Additionally, on days with large temperature changes, the impedance change is large, and on days with small temperature changes, the impedance change is small. This effect of temperature on the impedance change can be interpreted in two ways. First, the impedance may have been observed to change as the tree's physiological phenomenon is activated by temperature, and second, it may be unrelated to the tree's physiological phenomenon and the impedance value may have been directly affected by temperature changes.

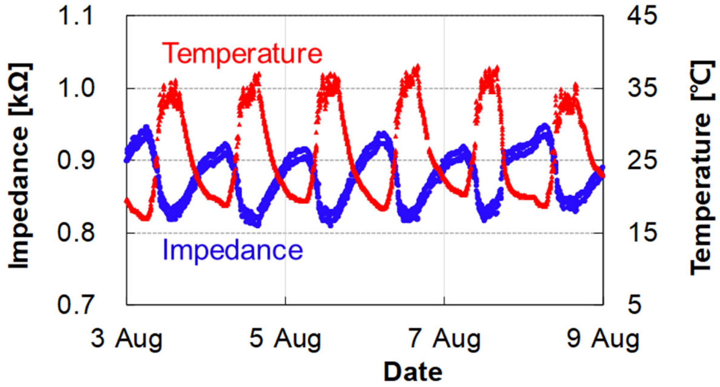

(**a**)

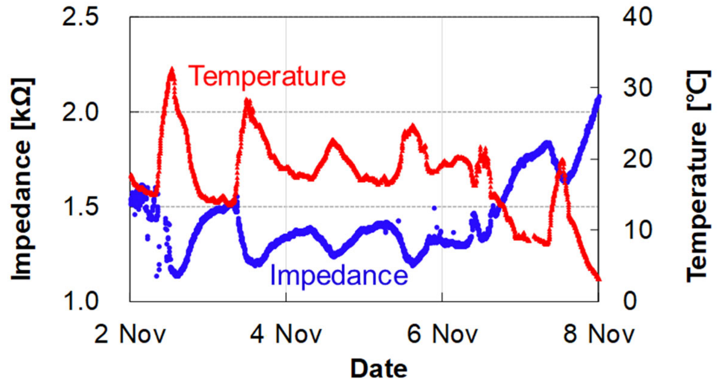

(**b**)

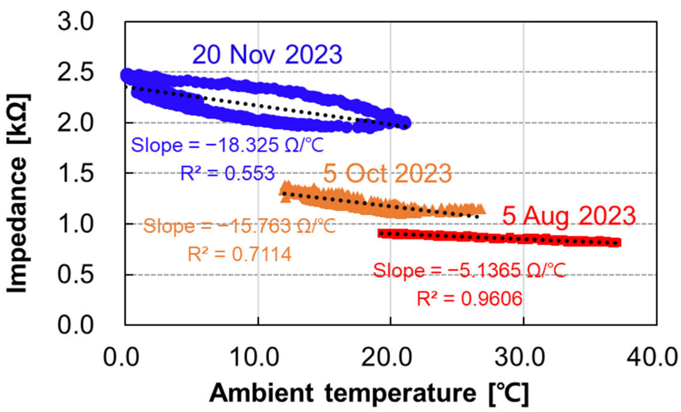

(**c**)

Figure 13. Graph of ambient temperature and impedance data: (**a**) when the leaves are lush, (**b**) without leaves, and (**c**) trajectory plot on a specific day.

In a previous study, Hyunjun P. observed a synchronized pattern between the temperature and electrical conductivity of paprika [21]. This is consistent with the observation that the impedance of zelkova trees growing outdoors is inversely proportional to temperature, as shown in Figure 13a. Hyunjun P. also measured the relative humidity as well as the impedance according to the temperature. When the impedance is low, the relative humidity is also low. However, the relative humidity has a flat shape of 60% in the evening and dawn, but drops to 20% in the morning and day, which is not synchronized with the change in the impedance.

Figure 13b shows the ambient temperature and impedance measurements when there are no leaves. The absence of any leaves means that the tree is not carrying out physiological activities, and the fluctuating impedance at this time cannot be said to be related to physiological activities. It seems desirable to interpret the tree impedance fluctuations when there are no tree leaves as being directly caused by changes in ambient temperature. Therefore, even when the leaves are in full bloom, the daily impedance fluctuations will include a mixture of the influence of the tree's physiological activation and the influence of changes in the ambient temperature.

Figure 13c is a graph plotting the ambient temperature on the x-axis and the impedance on the y-axis for a specific day. The closed loops formed at the bottom, middle, and top plot the intraday impedance change according to the intraday temperature change for one day in summer, fall, and winter, respectively. The characteristic of the summer trajectory (5 August) is that the impedance position is the lowest and shows a straight line with almost no hysteresis. The centrally located fall trajectory (5 October) has a mid-level impedance level and shows some hysteresis in the shape of the trajectory. The winter trajectory has a relatively large impedance, so it is located at the top, and the hysteresis is relatively large, so the trajectory shape is oval. Even in winter trajectories where all the leaves have fallen, the impedance shows fluctuations depending on the daily temperature ranges, so an analysis excluding the effects of the daily temperature ranges is necessary.

There have been previous research results that have observed changes in wood resistance depending on temperature or humidity. S. Mancuso measured the electrical resistance of excised olive tree tissue in response to temperature changes [22]. When the temperature was lowered from about 25 degrees to 10 degrees, there was a slight slope of resistance increase, and when the temperature was lowered from 10 degrees to -20 degrees, the resistance clearly increased linearly. As reported in the previous paper using wood specimens, hysteresis in the resistance trace was also reported when the temperature was lowered and then raised again. In Figure 13c, the data on 5 August 2023, measured from a tree growing outdoors, belong to the high-temperature region, and the impedance change in response to temperature changes is weak, as was the trend in the high-temperature region in the previous study. In the data from 20 November 2023 in Figure 13c, the change in the impedance in response to the temperature change shows hysteresis, as in the previous study.

Figure 14 shows a plot of the tree impedance values at daily ambient temperatures of 15 degrees, 20 degrees, and 25 degrees from 1 September to 30 November. In Figure 13b, impedance fluctuations were observed under the influence of ambient temperature even in the absence of tree leaves. Therefore, in order to exclude the influence of intraday temperature fluctuations and investigate impedance changes due to seasonal changes, the data for specific temperatures were graphed. The impedance data at 25 degrees, 20 degrees, and 15 degrees are marked with squares, triangles, and circles, respectively. Whether based on 15 degrees, 20 degrees, or 25 degrees, the impedance value tends to gradually increase linearly as the season changes. The slope of the increase in the impedance as the day goes by appears to be generally similar, specifically showing a slope of 8.4 Ω/day at 25 degrees, 9.7 Ω/day at 20 degrees, and 11.9 Ω/day at 15 degrees. Therefore, over 50 days, the impedance values extracted from 25 degrees, 20 degrees, and 15 degrees showed increases of approximately 420 Ω, 485 Ω, and 595 Ω, respectively. It can be seen that the lower the extraction temperature, the greater the impedance change. By comparing the impedance values over time at the same temperature, the effect of temperature could be ruled out. When the effect of temperature is excluded, it can be seen that the impedance of the tree has a linear relationship with the electrical impedance value as the season changes. It is a known fact that trees' physiological activity, which is active in the summer, decreases as winter approaches. It was revealed through the measurement data that the impedance values of the trees extracted at the same temperature have a linear correlation with the season. The R^2 value (coefficient of determination), which indicates that the closer it is to 1, the closer it is to the linear fit line, was calculated to be 0.89, 0.77, and 0.86 at 25 degrees, 20 degrees, and 15 degrees, respectively. Therefore, it is inferred that the impedance value of a tree extracted at the same temperature can be an indicator of the tree's physiological activity.

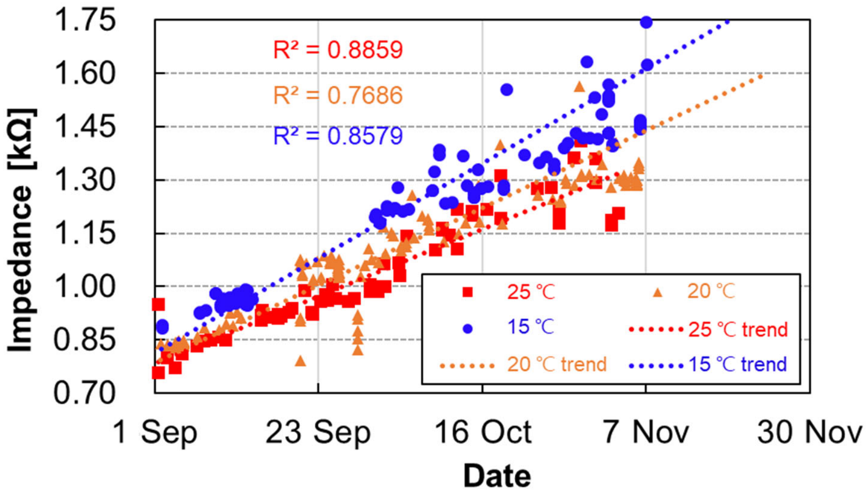

Figure 14. Impedance change at constant temperature according to seasonal changes.

Among previous studies, there has been an example of using the resistance value of wood at a certain temperature. Gagnon R., when using the resistance value of wood measured using a Shigometer, also measured the temperature and converted the measured resistance to a corrected resistance value at 15 degrees using pre-prepared temperature correction data [23]. This is consistent with the need for temperature compensation in previous studies, as Figure 13 shows a change in the impedance of the tree due to temperature changes even after all the leaves have fallen. In previous studies, resistance values measured at different temperatures were corrected and used, but in Figure 14, there was an impedance value measured directly at the corresponding temperature, so there was no need for correction.

Figure 15 is a plot showing the maximum light intensity during the day as the season changes. As the seasons change, the impedance value gradually increases, but no particular trend can be seen in the light intensity. Figure 16 shows the correlation between the light intensity and impedance on specific days in summer, fall, and winter. In the linear fit between the light intensity and impedance, it was determined that there was no correlation as the R^2 value was as low as 0.016.

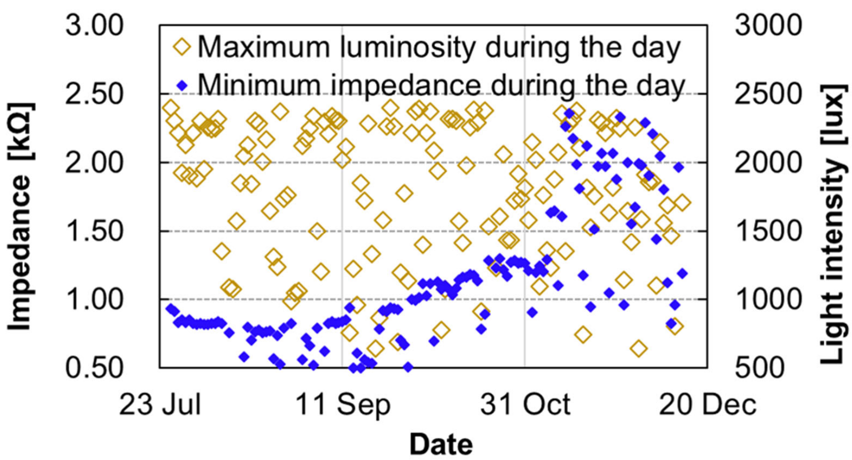

Figure 15. Ambient light intensity and impedance change with seasonal changes.

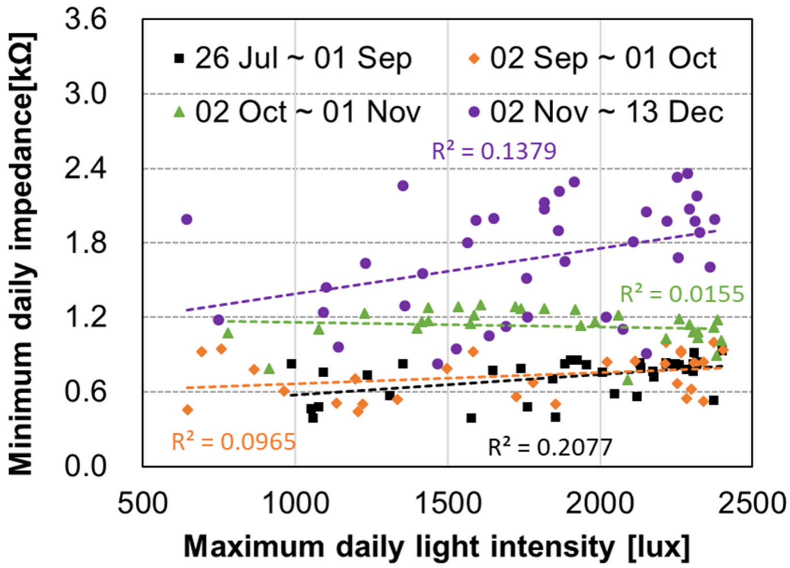

Figure 16. Correlation between light intensity and impedance at a specific date.

5. Conclusions

A TPAM system was developed to remotely, continuously, and quantitatively monitor the physiological activity of trees. The developed TPAM system also measures the ambient temperature and light intensity and wirelessly transmits the measured data to the hub system through ZigBee communication. Previous studies using plant electrical impedance measurements have used a two-contact measurement method, which includes errors due to the contact impedance of the electrodes. To improve the error of the two-contact measurement method, the TPAM system adopted a four-contact measurement method and measured the impedance of the trees according to seasonal changes over a long period of time. The impedance of the tree showed a periodic fluctuation cycle on a daily basis in the short term and tended to increase as the season changed from summer to winter in the long term. The shape of the impedance changes on a daily basis showed a shape that reversed the change in the ambient temperature. Even in winter, when there were no tree leaves, fluctuations in the tree impedance were observed according to the daily temperature changes. Since the absence of leaves means that the tree's physiological activity is at its lowest, the daily impedance fluctuations at this time are presumed to be a direct effect of ambient temperature fluctuations that are unrelated to the tree's physiological activity. The direct impact of these temperature fluctuations on tree impedance fluctuations will also affect the presence of tree leaves. Excluding the influence of temperature, the impedance values at constant temperatures of 15 degrees, 20 degrees, and 25 degrees were analyzed to determine the relationship between the impedance and physiological activity of the tree. As a result of analyzing the impedance value when the temperature was 25 degrees every day, it was found that the impedance value increased linearly with a slope of 8.4 Ω/day from summer to winter. The conclusion from this series of analyses is that in order to understand the physiological activities of trees, it is important to exclude the influence of temperature by continuously measuring the ambient temperature as well as measuring the impedance.

In the future, the following additional monitoring and system supplementation work will be needed. This paper reports monitoring results for the period from summer to early winter, but monitoring should also be performed for the period from late winter to spring and summer. The monitoring of multiple individuals of the same breed is necessary, as well as the monitoring of different breeds using the TPAM system. Additionally, the TPAM system must be equipped with a humidity measurement function. It is also necessary to examine whether humidity is related to tree growth and physiological activity. Currently, the system is constructed using commercial parts, resulting in high power consumption.

Because the measurements must be performed over several months, TPAM systems require low power consumption. An application-specific integrated circuit (ASIC) that can achieve a low power consumption are currently under development.

Author Contributions: J.K. produced HW. J.L. performed FW and SW coding, measurements, data processing, and drafted the paper. J.P.K. contributed to funding, paper idea, research progress, paper organization, and paper modification. All authors have read and agreed to the published version of the manuscript.

Funding: This paper was supported by the Education and Research promotion program of KOREATECH in 2023. This paper was supported by the Korea Institute for Advancement of Technology (KIAT) grant funded by the Korea Government (MOTIE) (P0008458, The Competency Development Program for Industry Specialist, 2023).

Institutional Review Board Statement: Not applicable.

Informed Consent Statement: Not applicable.

Data Availability Statement: The data presented in this paper are available from the corresponding author on reasonable request.

Acknowledgments: The authors thank the Cooperative Equipment Center at KOREATECH for assistance with FE-SEM analysis.

Conflicts of Interest: The authors declare no conflict of interest.

References

1. Johnstone, D.; Tausz, M.; Moore, G.; Nicolas, M. Chlorophyll fluorescence of the trunk rather than leaves indicates visual vitality in *Eucalyptus saligna*. *Trees Struct. Funct.* **2012**, *26*, 1565–1576. [CrossRef]
2. Sepúlveda, P.; Johnstone, D.M. A novel way of assessing plant vitality in urban trees. *Forests* **2019**, *10*, 2. [CrossRef]
3. Shortle, W.; Shigo, A.; Berry, P.; Abusamra, J. Electrical resistance in tree cambium zone: Relationship to rates of growth and wound closure. *For. Sci.* **1977**, *23*, 326–329.
4. Park, S.U.; Hong, Y.S. A study on the evaluation of woody tree vitality of artificial ground: Case study of seoullo 7017. *J. People Plants Environ.* **2021**, *24*, 85–94. [CrossRef]
5. Hirose, Y.; Sagawa, J.; Sibamoto, Y.; Kukita, Y. Coping with electrode polarization for development of DC-driven electrical impedance tomography. *Flow. Meas. Instrum.* **2021**, *81*, 102006. [CrossRef]
6. Muramatsu, N.; Hiraoka, K. Electrical impedance of fruit tree shoots from late winter to spring. *Environ. Control Biol.* **2006**, *44*, 77–83. [CrossRef]
7. Rafael, F.M.; Antonio, J.O.; Raman, G.G.; Irineo, T.; Gilberto, H.; Luis, M.C.; Juan, P.; Rosalia, V.O. An analysis of electrical impedance measurements applied for plant N status estimation in lettuce (*Lactuca sativa*). *Sensors* **2014**, *14*, 11492–11503.
8. Astashev, M.E.; Konchekov, E.M.; Kolik, L.V.; Gudkov, S.V. Electric impedance spectroscopy in trees condition analysis: Theory and experiment. *Sensors* **2022**, *22*, 8310. [CrossRef]
9. Serrano-Finetti, E.; Castillo, E.; Alejos, S.; León Hilario, L.M. Toward noninvasive monitoring of plant leaf water content by electrical impedance spectroscopy. *Comput. Electron. Agric.* **2023**, *210*, 107907. [CrossRef]
10. Meiqing, L.; Jinyang, L.; Hanping, M.; Yanyou, W. Diagnosis and detection of phosphorus nutrition level for solanum lycopersicum based on electrical impedance spectroscopy. *Biosyst. Eng.* **2016**, *143*, 108–118. [CrossRef]
11. Heaverbeke, M.V.; Stock, M.; De Baets, B. Equivalent electrical circuits and their use across electrochemical impedance spectroscopy application domains. *IEEE Access* **2022**, *10*, 51363–51379. [CrossRef]
12. Hayden, R.I.; Moyse, C.A.; Calder, F.W.; Crawford, D.P.; Fensom, D.S. Electrical impedance studies on potato and alfalfa tissue. *J. Exp. Bot.* **1969**, *20*, 177–200. [CrossRef]
13. Franks, W.; Schenker, I.; Schmutz, P.; Hierlemann, A. Impedance characterization and modeling of electrodes for biomedical applications. *IEEE Tran. Biomed. Eng.* **2005**, *52*, 1295–1302. [CrossRef]
14. Magar, H.S.; Hassan, R.Y.A.; Mulchandani, A. Electrochemical impedance spectroscopy (EIS): Principles, construction, and biosensing applications. *Sensors* **2021**, *21*, 6578. [CrossRef]
15. Amini, M.; Hisdal, J.; Kalvøy, H. Applications of bioimpedance measurement techniques in tissue engineering. *J. Electr. Bioimp.* **2018**, *9*, 142–158. [CrossRef]
16. Cosoli, G.; Mobili, A.; Tittarelli, F.; Revel, G.M.; Chiariotti, P. Electrical resistivity and electrical impedance measurement in mortar and concrete elements: A systematic review. *Appl. Sci.* **2020**, *10*, 9152. [CrossRef]
17. Wang, S.; Zhang, J.; Gharbi, O. Electrochemical impedance spectroscopy. *Nat. Rev. Methods Primers* **2020**, *41*, 1.
18. Miccoli, I.; Edler, F.; Pfnür, H.; Tegenkamp, C. The 100th anniversary of the four-point probe technique: The role of probe geometries in isotropic and anisotropic systems. *J. Phys.* **2015**, *27*, 223201. [CrossRef]

19. Aćimović, S.G.; Cregg, B.M.; Sundin, G.W.; Wise, J.C. Comparison of drill- and needle-based tree injection technologies in healing of trunk injection ports on apple trees. *Urban. For. Urban. Green.* **2016**, *19*, 151–157. [CrossRef]
20. Tomas, M.T.; Watson, W.T.; Arnold, M.A.; Lombardini, L.; Appel, D.N. Comparing various techniques to measure tree vitality of live oaks. *Urban. For. Urban. Green.* **2010**, *9*, 199–203.
21. Park, H.; Son, J.E.; Ahn, T.I.; Park, K.S.; Park, J.H. Nondestructive measurement of paprika (*Capsicum annuum* L.) internal electrical conductivity and its relation to environmental factors. *Korean J. Hortic. Sci. Technol.* **2018**, *36*, 691–701. [CrossRef]
22. Mancuso, S. Electrical resistance changes during exposure to low temperature measure chilling and freezing tolerance in olive tree (*Olea europaea* L.) plants. *Plant Cell Environ.* **2000**, *23*, 291–299. [CrossRef]
23. Gagnon, R.R.; Bauce, E.; Pineau, M. Relation between air water potential and cambial electrical resistance of balsam fir and white spruce after budbreak. *Can. J. For. Res.* **1987**, *17*, 105–108. [CrossRef]